

Baselining Network-Wide Traffic by Time-Frequency Constrained Stable Principal Component Pursuit

Kai Hu, and Zhe Wang

Abstract—In this letter, we develop a novel network-wide traffic analysis methodology, named Stable Principal Component Pursuit with Time-Frequency Constraints (SPCP-TFC), for extracting the baseline of a traffic matrix. Following a refined traffic matrix decomposition model, we present new time-frequency constraints to extend Stable Principal Component Pursuit (SPCP), and design an efficient numerical algorithm for SPCP-TFC. At last, we evaluate the SPCP-TFC method by abundant simulations, and show it has superior performance than other traffic baseline methods such as RBL and PCA.

Index Terms—baseline of traffic matrix, robust PCA, time-frequency constraint, numerical algorithm, simulation.

I. INTRODUCTION

THE Internet traffic data, which is usually modeled by the superposition of diverse components [1][2][3], is of critical importance to network management. The baseline traffic represents the most prominent traffic patterns [2], and is helpful to anomaly detection, capacity planning, and green computing. Most traditional studies focused on baselining the single-link traffic [4], however, as the network-wide traffic analysis is becoming increasingly popular, baselining the network-wide traffic turns into a most urgent problem.

The traffic matrix is an important kind of network-wide traffic data and has complex characteristics. The baseline of a traffic matrix should capture the common patterns among traffic flows, and be stable against the disturbance of large anomalies. Principal Component Analysis (PCA) was used for traffic matrix analysis in [1], and showed the low-rank nature of the baseline (i.e. the deterministic) component, but it performed poorly in the presence of contamination by large anomalies [5]. Recently, the Robust Principal Component Analysis (RPCA) theory [6] has attracted wide attentions. Supposing a low-rank matrix is contaminated by a sparse matrix whose non-zeros entries may have large magnitudes, Candès et al. [6] presented a robust matrix decomposition method named Principal Component Pursuit (PCP), and proved that under surprising board conditions, PCP could recover the low-rank matrix with high probability. Following this exact "low-rank and sparsity" assumption, Bandara et al. [2] proposed the Robust BaseLine (RBL) method, and argued that RBL performs better than several existing traffic baseline methods.

Intuitively, the baseline traffic time-series of each flow should be "smooth" enough, i.e. it records the long-term and

steady traffic trends (such as the diurnal pattern) and neglects the short-term fluctuations. However, to the best of our knowledge, this problem has not been adequately studied when baselining the traffic matrix. Actually, the resulting baseline traffic time-series for RBL are not smooth enough, and it can be explained that the empirical traffic matrix does not exactly meet the "low-rank and sparsity" assumption, on the contrary, it also contains non-smooth noisy fluctuations which should be decomposed specially. Furthermore, the evaluation of traffic baseline methods was not sufficient in previous studies. A key point is that obtaining the ground-truth baseline of real-world traffic data is usually impossible, consequently, one could neither measure the accuracy of a baseline method, nor compare the performances of different baseline methods. Therefore, baselining network-wide traffic is still a challenging task.

In this letter, we first establish a refinement of the traffic matrix decomposition model in [3], which extends the assumption of deterministic traffic matrix to characterize the smoothness of baseline traffic. Secondly, we propose a novel baseline method for the traffic matrix data, which solves a constrained convex program named Stable Principal Component Pursuit with Time-Frequency Constraints (SPCP-TFC). As an extension of the Stable Principal Component Pursuit (SPCP) method [7], SPCP-TFC takes distinctive time-frequency constraints for our refined model. Thirdly, we design the Accelerate Proximal Gradient (APG) algorithm for SPCP-TFC which has a fast convergence rate. At last, we evaluate our traffic baseline method by abundant simulations, and show it has a superior performance than RBL and PCA.

II. METHODOLOGY

A. A Refined Traffic Matrix Decomposition Model

Suppose $X \in \mathbb{R}^{T \times P}$ is a traffic matrix, and each column $X_j \in \mathbb{R}^T$ ($1 \leq j \leq P$) is a traffic flow in T time intervals. A traffic flow is the traffic of a Original-Destination (OD) pair [1], or the traffic traversing a unidirectional backbone link [2]. In [3], we proposed the simple Traffic Matrix Decomposition Model (TMDM), assuming X is the sum of a low-rank matrix, a sparse matrix, and a noise matrix. This model is equivalent to the data model of the generalized RPCA problem [7], and the low-rank deterministic traffic matrix corresponds to the baseline traffic¹. However, TMDM gives no temporal characteristics of the baseline traffic. Since each baseline traffic flow records the long-term and steady traffic trends, it should display a smooth curve. Plenty of mathematical tools, such as

¹In the following discussion, the words "deterministic traffic" and "baseline traffic" are used interchangeably.

wavelets and splines, can formulate smoothness. As the most salient baseline traffic patterns are slow oscillation behaviors, this letter formulates the baseline traffic time-series as the sum of harmonics with low frequencies, and establishes a Refined Traffic Matrix Decomposition Model (R-TMDM):

Definition 1 (R-TMDM) *The traffic matrix $X \in \mathbb{R}^{T \times P}$ is the superposition of the deterministic (baseline) traffic matrix A , the anomaly traffic matrix E , and the noise traffic matrix N . A is a low-rank matrix, and for each column time-series in A , the Fourier spectra whose frequencies exceed a critical value f_c are zeros; E is a sparse matrix, but the non-zeros entries may have large magnitudes; N is a random noise matrix, and each column time-series is a zero-mean stationary random process.*

For simplicity, we assume each column N_j ($1 \leq j \leq P$) is the white Gaussian noise with variance $\sigma_j^2 > 0$ in this letter.

B. Stable Principal Component Pursuit with Time-Frequency Constraints

Stable Principal Component Pursuit (SPCP) for the generalized RPCA problem solves this convex program [7]:

$$\begin{aligned} & \underset{A, E, N}{\text{minimize}} \|A\|_* + \lambda \|E\|_1 \\ & \text{s.t. } A + E + N = X, \quad \|N\|_F^2 \leq \delta, \end{aligned} \quad (1)$$

where $\|\cdot\|_*$, $\|\cdot\|_1$, $\|\cdot\|_F$ denote the nuclear norm, the l_1 norm, and the Frobenius norm, respectively; $\lambda > 0$ is the balance parameter, and $\delta > 0$ is the constraint parameter. To extract the baseline traffic more powerfully, we extend SPCP by preserving the objective function and redesigning the constraint functions.

Firstly, considering the R-TMDM model, it is necessary to add a constraint for the baseline traffic matrix based on its frequency-domain assumption. $W = [W_0 \cdots W_{T-1}]_{T \times T}$ denotes the discrete Fourier basis matrix of length T . For each $0 \leq k \leq T-1$, the Fourier basis W_k is defined as

$$W_k(t) = \frac{1}{\sqrt{T}} e^{-i \frac{2\pi k}{T} (t-1)}, \quad t = 1, \dots, T, \quad (2)$$

with frequency $f_k = \min\{\frac{k}{T}, \frac{T-k}{T}\}$. W_H is made up of the high-frequency bases W_k satisfying $f_k \geq f_c$, thus $W_H(W_H)^\top$ is the projection matrix to high-frequency subspace. We use the following constraint for the baseline traffic matrix:

$$W_H(W_H)^\top A = 0_{T \times P}. \quad (3)$$

Secondly, unlike the Frobenius norm inequality in (1), we use a different constraint strategy for the noise traffic. For each column vector N_j ($1 \leq j \leq P$), consider its periodogram $\{I_{N_j}(f_k)\}_{k=0}^{T-1}$ for the Fourier frequencies $\{f_k\}_{k=0}^{T-1}$:

$$I_{N_j}(f_k) = |W_k^\top N_j|^2 = \left| \frac{1}{\sqrt{T}} \sum_{t=1}^T N_j(t) e^{-i \frac{2\pi k}{T} (t-1)} \right|^2. \quad (4)$$

χ_s^2 (χ_s) denotes the Chi-square (Chi) distribution with s freedom degree, and it is well-known [8] that when N_j are i.i.d. standard Gaussian variables², $\{2I_{N_j}(f_k)\}_{k=1}^{T-1}$ are

i.i.d χ_2^2 variables, and $I_{N_j}(f_0)$ is a χ_1^2 variable. Therefore, $\{\sqrt{2}|W_k^\top N_j|\}_{k=1}^{T-1}$ are i.i.d χ_2 variables, and $|W_0^\top N_j|$ is a χ_1 variable. We choose these time-frequency constraints for the noise traffic matrix:

$$\begin{cases} \sqrt{2} \|[W_1 \cdots W_{T-1}]^\top N_j\|_\infty \leq \delta_1, \\ |W_0^\top N_j| \leq \delta_2, \\ \|N_j\|_\infty \leq \delta_3, \end{cases} \quad j = 1, \dots, P. \quad (5)$$

Equivalently, N lies in the convex subset $B(\delta_1, \delta_2, \delta_3)$:

$$B(\delta_1, \delta_2, \delta_3) \triangleq \left\{ N \mid N \in \mathbb{R}^{T \times P} \text{ and satisfies } (5) \text{ with } \delta_1, \delta_2, \delta_3 > 0 \right\}. \quad (6)$$

The main idea of (5) is to eliminate the low-frequency baseline traffic from the resulting noise traffic by utilizing the value distribution of its periodogram, while the Frobenius norm constraint in (1) could not filter the baseline traffic so efficiently.

Lastly, using the new constraints (3) and (5), we propose our traffic baseline method, named Stable Principal Component Pursuit with Time-Frequency Constraints (SPCP-TFC):

$$\begin{aligned} & \underset{A, E, N}{\text{minimize}} \|A\|_* + \lambda \|E\|_1 \\ & \text{s.t. } A + E + N = X, \quad W_H(W_H)^\top A = 0_{T \times P}, \\ & \quad N \in B(\delta_1, \delta_2, \delta_3), \end{aligned} \quad (7)$$

which outputs A as the baseline traffic matrix. In this study, we set $\delta_1 = 3.03$, $\delta_2 = \delta_3 = 2.56$, corresponding to the 99% confidence intervals of the χ_2 , χ_1 , and Gaussian variables, respectively.

C. Numerical Algorithm

SPCP-TFC solves a constrained program which is computational expensive. The Accelerate Proximal Gradient (APG) algorithm considers this relaxed unconstrained program:

$$\begin{aligned} & \underset{A, E, N}{\text{minimize}} F(A, E, N) \triangleq \mu g(A, E, N) + f(A, E, N) \\ & f(A, E, N) \triangleq \frac{1}{2} \|X - A - E - N\|_F^2 + \frac{\beta}{2} \|W_H(W_H)^\top A\|_F^2 \\ & g(A, E, N) \triangleq \|A\|_* + \lambda \|E\|_1 + \iota_{B(\delta_1, \delta_2, \delta_3)}(N) \end{aligned} \quad (8)$$

The function $f(A, E, N)$, which is convex and differentiable, penalizes violations of the two equality constraints in (7), and $\beta > 0$ is a balancing parameter. $g(X, E, N)$ is a linear combination of three convex but non-differentiable functions. $\mu > 0$ is a relaxation parameter, as $\mu \searrow 0$, the solution to (8) approaches to the solution to (7). ∇f denotes the gradient of f , which equals to

$$\nabla f(A, E, N) = \begin{bmatrix} [I + \beta W_H(W_H)^\top] A + E + N - X \\ A + E + N - X \\ A + E + N - X \end{bmatrix}$$

and is Lipschitz continuous by the following proposition.

Proposition 1: $\nabla f(A, E, N)$ is Lipschitz continuous, and the Lipschitz constant is $L = \sqrt{9 + 4\beta + \beta^2}$.

For the proof, see the appendix section.

Instead of directly minimizing $F(A, E, N)$, the APG algorithm minimizes a sequence of quadratic approximations,

²As the preprocessing for X , for each column vector X_j ($1 \leq j \leq P$), we divide it by σ_j . This operation normalizes the Gaussian variables in N , and preserves all the hypotheses of A and E in the R-TMDM model.

denoted as $Q(A, E, N, Y^A, Y^E, Y^N)$, of $F(A, E, N)$ at a specially chosen point (Y^A, Y^E, Y^N) (renewed in each step):

$$\begin{aligned} & Q(A, E, N, Y^A, Y^E, Y^N) \\ &= \mu g(A, E, N) + f(Y^A, Y^E, Y^N) \\ & \quad \langle \nabla f(Y^A, Y^E, Y^N), (A, E, N) - (Y^A, Y^E, Y^N) \rangle + \\ & \quad \frac{L}{2} \|(A, E, N) - (Y^A, Y^E, Y^N)\|_F^2. \end{aligned} \quad (9)$$

It can be derived that

$$\begin{aligned} & \underset{A, E, N}{\text{minimize}} Q(A, E, N, Y^A, Y^E, Y^N) \\ &= \underset{A}{\text{minimize}} \left\{ \mu \|A\|_* + \frac{L}{2} \|A - G^A\|_F^2 \right\} + \\ & \underset{E}{\text{minimize}} \left\{ \mu \lambda \|E\|_1 + \frac{L}{2} \|E - G^E\|_F^2 \right\} + \\ & \underset{N}{\text{minimize}} \left\{ \mu \iota_{B(\delta_1, \delta_2, \delta_3)}(N) + \frac{L}{2} \|N - G^N\|_F^2 \right\} + \text{Constant} \end{aligned} \quad (10)$$

where

$$\begin{cases} G^A = Y^A - \frac{1}{L} ([I + \beta W_H(W_H)^\top] Y^A + Y^E + Y^N - X) \\ G^E = Y^E - \frac{1}{L} (Y^A + Y^E + Y^N - X) \\ G^N = Y^N - \frac{1}{L} (Y^A + Y^E + Y^N - X) \end{cases}$$

Thus (10) splits into three subproblems, which are equivalent to the *proximity operators* associated with the convex functions $\frac{\mu}{L} \|A\|_*$, $\frac{\mu \lambda}{L} \|E\|_1$, and $\frac{\mu}{L} \iota_{B(\delta_1, \delta_2, \delta_3)}(N)$, respectively. Using basic results in [11], they have explicit solutions as follow:

$$\arg \min_A \left\{ \mu \|A\|_* + \frac{L}{2} \|A - G^A\|_F^2 \right\} = U \mathcal{S}_{\frac{\mu}{L}}[\Sigma] V^\top, \quad (11)$$

$$\arg \min_E \left\{ \mu \lambda \|E\|_1 + \frac{L}{2} \|E - G^E\|_F^2 \right\} = \mathcal{S}_{\frac{\mu \lambda}{L}}[G^E], \quad (12)$$

$$\arg \min_N \left\{ \mu \iota_{B(\delta_1, \delta_2, \delta_3)}(N) + \frac{L}{2} \|N - G^N\|_F^2 \right\} = \mathcal{P}_{B(\delta_1, \delta_2, \delta_3)}[G^N], \quad (13)$$

where $U \Sigma V^\top$ is the singular value decomposition (SVD) of G^A , $\mathcal{P}_{B(\delta_1, \delta_2, \delta_3)}$ is the projection operator to $B(\delta_1, \delta_2, \delta_3)$, and \mathcal{S}_ϵ is the soft-thresholding operator with parameter ϵ [3]. For each $X \in \mathbb{R}^{T \times P}$, $\mathcal{S}_\epsilon[X] \in \mathbb{R}^{T \times P}$ and it satisfies

$$\mathcal{S}_\epsilon[X](i, j) \triangleq \text{sign}(X(i, j)) \max\{|X(i, j)| - \epsilon, 0\}.$$

Algorithm 1 presents the APG algorithm for SPCP-TFC, moreover, the following theorem proves that Algorithm 1 has the $O(1/k^2)$ convergence rate. Since the proof of this theorem is quite close to Theorem 4.4 in [10], we omit it and directly summarize this result:

Theorem 1 Let $F(A, E, N) = \bar{\mu} g(A, E, N) + f(A, E, N)$. Then for all $k > k_0 = \left\lceil \log\left(\frac{\mu_0}{\bar{\mu}}\right) / \log\left(\frac{1}{\eta}\right) \right\rceil$, we have

$$F(X_k) - F(X^*) \leq \frac{2\sqrt{9 + 4\beta + \beta^2} \|X_{k_0} - X^*\|_F^2}{(k - k_0 + 1)^2}, \quad (14)$$

where $X_k = (A_k, E_k, N_k)$ is defined in Algorithm 1, and $X^* = (A^*, E^*, N^*)$ is a solution to (8) when $\mu = \bar{\mu}$.

Algorithm 1 APG for SPCP-TFC

Input: traffic matrix $X \in \mathbb{R}^{T \times P}$.

Normalization: $X = X / \text{diag}\{\sigma_j\}$.

Initialization: $A_0 = A_{-1} = E_0 = E_{-1} = N_0 = N_{-1} = 0$; $t_0 = t_{-1} = 1$; $k = 0$. $\mu_0 = 0.99 \|X\|_2$; $\bar{\mu} = 10^{-5} \mu_0$; $\eta = 0.9$. $L = \sqrt{9 + 4\beta + \beta^2}$; $\lambda = 1 / \sqrt{\max(T, P)}$.

While not converged **do**

$$Y_k^A = A_k + \frac{t_{k-1}-1}{t_k} (A_k - A_{k-1});$$

$$Y_k^E = E_k + \frac{t_{k-1}-1}{t_k} (E_k - E_{k-1});$$

$$Y_k^N = N_k + \frac{t_{k-1}-1}{t_k} (N_k - N_{k-1});$$

$$G_k^A = Y_k^A - \frac{1}{L} ([I + \beta W_H(W_H)^\top] Y_k^A + Y_k^E + Y_k^N - X);$$

$$G_k^E = Y_k^E - \frac{1}{L} (Y_k^A + Y_k^E + Y_k^N - X);$$

$$G_k^N = Y_k^N - \frac{1}{L} (Y_k^A + Y_k^E + Y_k^N - X);$$

$(U, S, V) = \text{svd}[G_k^A]$; // Singular Value Decomposition.

$$A_{k+1} = U \mathcal{S}_{\frac{\mu}{L}}[S] V^\top; E_{k+1} = \mathcal{S}_{\frac{\lambda \mu}{L}}[G_k^E];$$

$$N_{k+1} = \mathcal{P}_{B(\delta_1, \delta_2, \delta_3)}[G_k^N];$$

$$t_{k+1} = (1 + \sqrt{4t_k^2 + 1})/2; \mu_{k+1} = \max(\eta \mu_k, \bar{\mu});$$

$$k = k + 1.$$

End while

Output: $A = A_k \cdot \text{diag}\{\sigma_j\}$ is the baseline traffic matrix.

III. SIMULATION RESULTS

We evaluate SPCP-TFC by simulated traffic matrices, because the simulation approach could provide the ground-truth baseline data, perform abundant experiments independently, and change parameters to verify an algorithm's stability. Consequently, we first introduces the simulation techniques.

Suppose the network has 10 nodes, the measurement window is one week, and the minimal time interval is $\Delta t = 5$ minutes. Under this setting, each traffic matrix $X \in \mathbb{R}^{T \times P}$ has $P = 10^2 = 100$ OD flows in $T = 7 \times 24 \times 12 = 2016$ time intervals, and it is generated by the following three traffic components. (1) For each flow j , the baseline traffic A_j is the sum of a content $a_{j,0}$ and a few *sin* functions:

$$A_j(t) = a_{j,0} + \sum_{m=1}^M a_{j,m} \sin\left(\frac{2\pi l_m t}{T} + \varphi_{j,m}\right), j = 1, \dots, P.$$

We assume that in each simulation, $\{a_{j,0}\}_{j=1}^P$ satisfies the gravity model and $\sum_{j=1}^P a_{j,0} = 10^6$. Since the period of the m -th *sin* is $\frac{T}{l_m} \times \frac{\Delta t}{60}$ hours, we choose $\{l_m\} = \{7, 14, 28, 56, 112\}$, and the periods of oscillation traffic are $\{24, 12, 6, 3, 1.5\}$ hours³. Moreover, the phase parameters $\{\varphi_{j,m}\}$ are uniform distributed in $[-\frac{\pi}{5}, \frac{\pi}{5}]$, and the amplitudes of the *sin* functions decay quickly as m increases by $a_{j,m+1} = 0.5 a_{j,m}$. (2) The non-zero entries are randomly distributed in 1% positions of the anomaly traffic matrix E , and for each flow j , the volume of each anomaly is $0.8 a_{j,0}$. (3) For each flow j , the noise traffic N_j consists of T independent Gaussian variables $N(0, \sigma_j^2)$, where $\sigma_j = \alpha a_{j,0}$, $\alpha > 0$ controls the noise rate.

We simulate 100 baseline traffic matrices simultaneously, and generate one anomaly traffic matrix and two noise traffic matrices for each of them (α is chosen as 0.1 and 0.2, which

³This setting is based on the discussions on backbone traffic in [1][5], for simplicity, we neglect periodical traffic patterns longer than 24 hours.

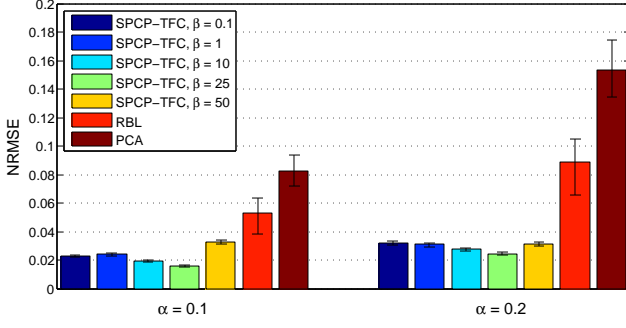


Fig. 1. The NRMSEs between the resulting and the ground-truth baseline traffic matrices. The bar shows the median and the error bar shows 10% and 90% percentile. Left group: $\alpha = 0.1$; right group: $\alpha = 0.2$.

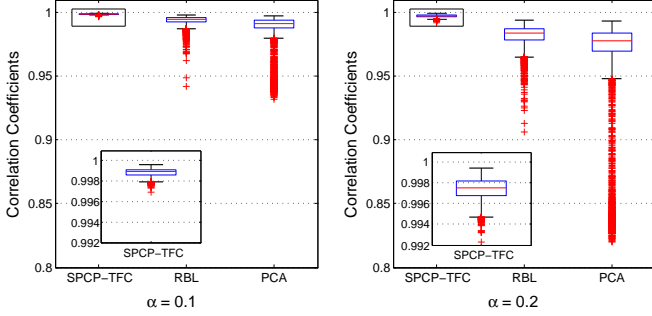


Fig. 2. Boxplots of the Pearson Correlation Coefficients between resulting and ground-truth baseline traffic flows. The results of SPCP-TFC are enlarged in small plots. Left panel: $\alpha = 0.1$; right panel: $\alpha = 0.2$.

means a low-level noise and a high-level noise, respectively). Therefore, 200 simulated traffic matrices are used in experiment. It can be verified that these matrices satisfy the R-TMDM model, and the critical frequency $f_c = \frac{112}{2016}$. SPCP-TFC is compared with other two network-wide traffic baseline methods: RBL [2] and PCA [1]. We apply these methods to the simulation dataset, and evaluate them by three metrics.

The first metric is the *Normalized Root Mean Squared Error* (NRMSE) between the ground-truth baseline traffic matrix A and its estimation \hat{A} :

$$\text{NRMSE} = \|A - \hat{A}\|_F / \|A\|_F. \quad (15)$$

Fig. 1 illustrates the NRMSEs of different baseline methods under two noise levels. For SPCP-TFC, we test different values of parameter $\beta \in \{0.1, 1, 10, 25, 50\}$. It can be observed that, SPCP-TFC archives significant lower NRMSEs than RBL and PCA, and this result is stable in a large range of β values. And our traffic baseline method shows the best performance when $\beta = 25$: under the low (high) noise level, the median of NRMSEs for SPCP-TFC is as 30.3%(27.3%) as that for RBL, and is as 19.5%(15.9%) as that for PCA. Hence we only consider SPCP-TFC with this fixed value in the following discussions.

The second metric characterizes the temporal correlation between each pair of ground-truth and resulting baseline traffic flows using their *Pearson Correlation Coefficient*. As a traffic matrix contains 100 flows, under each noise level, we compute $100 \times 100 = 10^4$ correlation coefficients for each baseline method. We display boxplots of these coefficients in Fig. 2. It is shown that the correlation coefficients for SPCP-TFC are very close to 1, and have an obviously greater median

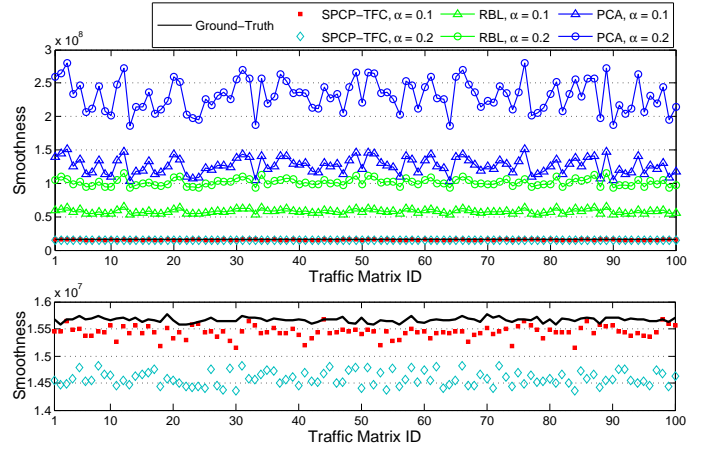


Fig. 3. The smoothness of resulting and ground-truth baseline traffic matrices. An enlarged view of SPCP-TFC's smoothness is shown in the bottom panel.

TABLE I
A COMPARISON BETWEEN DIFFERENT BASELINE METHODS ON THE NORMALIZED MEAN SMOOTHNESS VALUES

α	SPCP-TFC	RBL	PCA	Ground-Truth
0.1	0.99	3.72	8.10	1.00
0.2	0.95	6.48	14.78	1.00

than RBL and PCA. Thus the SPCP-TFC method extracts the temporal characteristics of the baseline traffic more precisely.

The third metric characterizes baseline traffic on smoothness, which adds up the *Total Variations* of the traffic flows in baseline traffic matrix. A small value of this metric indicates the traffic is sufficient smooth. Applying this metric to the baseline results aforementioned, we display the curve of 100 smoothness values (arranged by traffic matrix ID) for each baseline method, and for the 100 ground-truth values, in Fig. 3. We then compute the mean smoothness of each baseline method, and normalize it by dividing the mean smoothness of the ground-truth baseline traffic matrices. These normalized mean smoothness values (under two noise levels) are summarized in Tab. I. The estimated baseline traffic matrices by RBL and PCA are significantly more coarse than the ground-truth baseline traffic, and their mean smoothness values are larger than three times and eight times of the ground-truth value, respectively. Instead, the SPCP-TFC method leads to more accurate baseline estimations on smoothness. This is because the high-frequency traffic, which has larger total variation, can be successfully eliminated from the baseline by SPCP-TFC.

From Fig. 1-3 and Tab. I, we can also observe that when the noise rate α grows from 0.1 to 0.2, the performance of our baseline method shows a decline: the NRMSEs raise, the correlation coefficients drop down, and the smoothness values of resulting baseline traffic diverge from the ground-truth more evidently. This is mainly because the low-frequency component of the noise traffic, which could not be directly distinguished from the baseline traffic, is proportional to α .

IV. CONCLUSIONS

In this letter, we propose a refined traffic matrix decomposition model, and introduce a novel baseline method for traffic matrix named SPCP-TFC, which extends SPCP by using new

constraint functions for the baseline traffic and the noise traffic, respectively. We design an APG algorithm for SPCP-TFC, whose convergence rate is $O(1/k^2)$. Our baseline method is demonstrated by abundant simulations. Using three distinct metrics to evaluate the baseline results, we show SPCP-TFC has a superior performance than RBL and PCA.

REFERENCES

- [1] A. Lakhina, K. Papagiannaki, M. Crovella, C. Diot, E. D. Kolaczyk, and N. Taft. Structural analysis of network traffic flows. *SIGMETRICS Perform. Eval. Rev.* vol. 32, no. 1, pp. 61-72, June 2004.
- [2] V. W. Bandara and A. P. Jayasumana. Extracting Baseline Patterns in Internet Traffic Using Robust Principal Components. *Proc. IEEE LCN*, 2011.
- [3] Z. Wang, K. Hu, K. Xu, B. Yin and X. Dong. Structural Analysis of Network Traffic Matrix via Relaxed Principal Component Pursuit. *Computer Networks*, vol. 56, no. 7, pp. 2049-2067, 2012.
- [4] H. Hajji. Baseline Network Traffic and Online Faults Detection. *Proc. IEEE ICC*, 2003.
- [5] B. Rubinstein, B. Nelson, L. Huang, A. Joseph, S. Lau, S. Rao, N. Taft and J. Tygar. ANTIDOTE: understanding and defending against poisoning of anomaly detectors. *Proc. ACM IMC*, 2009.
- [6] E. Candes, X. Li, Y. Ma, and J. Wright. Robust principal component analysis? *Journal of the ACM*, vol. 58, no. 3, pp. 1-37, 2011.
- [7] Z. Zhou, X. Li, J. Wright, E. Candes, and Y. Ma. Stable principal component pursuit. *Proc. IEEE ISIT*, 2010.
- [8] P. Kokoszka and T. Mikosch. The periodogram at the Fourier frequencies. *Stochastic Processes and their Applications*, vol. 86, no. 1, pp. 49-79, 2000.
- [9] Z. Lin, A. Ganesh, J. Wright, L. Wu, M. Chen and Y. Ma. Fast convex optimization algorithms for exact recovery of a corrupted low-rank matrix. *Proc. IEEE CAMSAP*, 2009.
- [10] A. Beck and M. Teboulle. A fast iterative shrinkage-thresholding algorithm for linear inverse problems. *SIAM Journal on Imaging Sciences*, vol. 2, no. 1, pp. 183-202, 2009.
- [11] P. L. Combettes and J.-C. Pesquet. Proximal splitting methods in signal processing. *Fixed-Point Algorithms for Inverse Problems in Science and Engineering*, pp. 185-212. Springer, New York, 2011.

APPENDIX A. PROOF OF PROPOSITION 1

Proof: For any two points (A_1, E_1, N_1) and (A_2, E_2, N_2) in $\mathbb{R}^{T \times P} \times \mathbb{R}^{T \times P} \times \mathbb{R}^{T \times P}$, we have

$$\begin{aligned}
& \|\nabla f(A_1, E_1, N_1) - \nabla f(A_2, E_2, N_2)\|_F^2 \\
&= \|[I + \beta W_H(W_H)^\top](A_1 - A_2) + (E_1 - E_2) + (N_1 - N_2)\|_F^2 \\
&\quad + 2\|(A_1 - A_2) + (E_1 - E_2) + (N_1 - N_2)\|_F^2 \\
&\leq \left(\beta \|W_H(W_H)^\top(A_1 - A_2)\|_F^2 + \|A_1 - A_2\|_F^2 + \|E_1 - E_2\|_F^2 \right. \\
&\quad \left. + \|N_1 - N_2\|_F^2\right)^2 + \\
&\quad 2\left(\|A_1 - A_2\|_F^2 + \|E_1 - E_2\|_F^2 + \|N_1 - N_2\|_F^2\right)^2 \\
&= \beta^2 \|W_H(W_H)^\top(A_1 - A_2)\|_F^2 + \\
&\quad 2\beta \left(\|W_H(W_H)^\top(A_1 - A_2)\|_F^2 \|A_1 - A_2\|_F^2 + \right. \\
&\quad \left.\|W_H(W_H)^\top(A_1 - A_2)\|_F^2 \|E_1 - E_2\|_F^2 + \right. \\
&\quad \left.\|W_H(W_H)^\top(A_1 - A_2)\|_F^2 \|N_1 - N_2\|_F^2\right) + \\
&\quad 3\left(\|A_1 - A_2\|_F^2 + \|E_1 - E_2\|_F^2 + \|N_1 - N_2\|_F^2\right) + \\
&\quad 6\left(\|A_1 - A_2\|_F \|E_1 - E_2\|_F + \|A_1 - A_2\|_F \|N_1 - N_2\|_F \right. \\
&\quad \left. + \|E_1 - E_2\|_F \|N_1 - N_2\|_F\right) \\
&\leq (3\beta + \beta^2) \|W_H(W_H)^\top(A_1 - A_2)\|_F^2 + \\
&\quad (9 + \beta) \left(\|A_1 - A_2\|_F^2 + \|E_1 - E_2\|_F^2 + \|N_1 - N_2\|_F^2\right). \tag{16}
\end{aligned}$$

As $W_H(W_H)^\top$ is a projection operator in \mathbb{R}^T , for each $p \in \{1, \dots, P\}$,

$$\|W_H(W_H)^\top[A_1(p) - A_2(p)]\| \leq \|A_1(p) - A_2(p)\|. \tag{17}$$

therefore, we have

$$\begin{aligned}
& \|W_H(W_H)^\top(A_1 - A_2)\|_F^2 = \\
&= \sum_{p=1}^P \|W_H(W_H)^\top[A_1(p) - A_2(p)]\|^2 \\
&\leq \sum_{p=1}^P \|A_1(p) - A_2(p)\|^2 = \|A_1 - A_2\|_F^2. \tag{18}
\end{aligned}$$

Add (18) to (16) and let $L = \sqrt{9 + 4\beta + \beta^2}$, we have

$$\begin{aligned}
& \|\nabla f(A_1, E_1, N_1) - \nabla f(A_2, E_2, N_2)\|_F^2 \\
&\leq (9 + 4\beta + \beta^2) \left(\|A_1 - A_2\|_F^2 + \|E_1 - E_2\|_F^2 + \|N_1 - N_2\|_F^2\right) \\
&= L \|(A_1, E_1, N_1) - (A_2, E_2, N_2)\|_F^2. \tag{19}
\end{aligned}$$

This completes the proof. \square